Liquid-liquid phase separation in secondary organic aerosol particles produced from α-pinene ozonolysis and α-pinene photo-oxidation with/without ammonia

Suhan Ham[1], Zaeem Bin Babar[2], Jaebong Lee[3], Hojin Lim[2], Mijung Song[1*]

[1] {Department of Earth and Environmental Sciences, Chonbuk National University, Jeonju, Jeollabuk-do, Republic of Korea}

[2] {Department of Environmental Engineering, Kyungpook National University, Daegu, Republic of Korea}

[3] {Thermal Hydraulics & Severe Accident Research Division, Korea Atomic Energy Research Institute, Daejeon, Republic of Korea}

Correspondence to: Mijung Song (mijung.song@jbnu.ac.kr)

Abstract

Recently, liquid–liquid phase separation (LLPS) of secondary organic aerosol (SOA) particles free of inorganic salts has been intensively studied because of their importance on cloud condensation nuclei (CCN) properties. Herein, we investigated LLPS in four different types of SOA particles generated from α-pinene ozonolysis and α-pinene photo-oxidation in the absence and presence of NH_3. LLPS was observed in SOA particles produced from α-pinene ozonolysis at ~95.8% relative humidity (RH) and α-pinene ozonolysis with NH_3 at ~95.4% RH. However, LLPS was not observed in SOA particles produced from α-pinene photo-oxidation and α-pinene photo-oxidation with NH_3. With datasets of average oxygen to carbon elemental ratio (O:C) for different types of SOA particles of this study and previous studies, there appears to be a relationship between the occurrence of LLPS and the O:C of the SOA particles. When LLPS was observed, the two liquid phases were present up to ~100% RH. This result can help to predict more accurate results of CCN properties of organic aerosol particles.

1 Introduction

Secondary organic (SOA) particles in the atmosphere can be formed by the oxidation of volatile organic compounds (VOCs) emitted from biogenic and anthropogenic sources (Hallquist et al., 2009). These SOA particles comprise ~20–80% of ultrafine aerosol particles depending on the location (Zhang et al., 2007; Jimenez et al., 2009). They can affect the energy balance of the Earth by scattering and absorbing solar radiation and also by acting as nuclei for cloud formation (Kanakidou et al., 2005; Hallquist et al., 2009; IPCC, 2013; Knopf et al., 2018). In addition, these particles can affect air quality and human health (Kanakidou et al., 2005; Jang et al., 2006; Solomon et al., 2007; Baltensperger et al., 2008; Murray et al., 2010; Wang et al., 2012; Poschl and Shiraiwa, 2015; Shiraiwa et al., 2017).

Many previous studies showed that SOA particles can be formed more efficiently in the presence of gaseous species such as ammonia (NH_3) (Zhang et al., 2004; Na et al., 2006; Na et al., 2007; Laskin et al., 2014; Liu et al., 2015a; Liu et al., 2015b; Babar et al., 2017). NH_3 is one of the abundant and reactive gaseous species in the atmosphere (Reis et al., 2009; Heald et al., 2012; Reche et al., 2015; Zheng et al., 2015; Sharma et al., 2016; Warner et al., 2016). The chemical composition of SOA particle can be influenced by the reaction with NH_3 (Laskin et al., 2015; Liu et al., 2015b), but it is still poorly understood.

Aerosol particles containing SOAs can undergo phase transitions in the atmosphere as relative humidity (RH) changes. So far, many researchers have focused on phase transitions, especially liquid–liquid phase separation (LLPS) in particles containing SOAs and inorganic salts during changes to RH (Pankow et al., 2003; Marcolli et al., 2006; Ciobanu et al., 2009; Bertram et al., 2011; Krieger et al., 2012; Song et al., 2012a; Song et al., 2012b; Zuend and Seinfeld., 2012; Ault et al., 2013; Veghte et al., 2013; O'Brien et al., 2015). They established that LLPS always occurred in SOA particles mixed with inorganic salts when the oxygen to carbon elemental ratio (O:C) of the organic materials is smaller than 0.56, while LLPS never occurred when the O:C of the organic materials is greater than 0.80. LLPS commonly occurred in the intermediate O:C ratio range (Bertram et al., 2011; Krieger et al., 2012; Song et al., 2012a; Song et al., 2013; You et al., 2013; You et al., 2014). LLPS in a mixture of SOA particles and inorganic salts is known to affect optical properties (Fard et al., 2018), gas–particle partitioning (Zuend et al., 2010; Zuend and Seinfeld, 2012; Shiraiwa et al., 2013), reactivity (Kuwata and Martin., 2012), hygroscopic properties (Hodas et al., 2016), and cloud condensation nuclei (CCN) properties

of these particles (Hodas et al., 2016; Ovadnevaite et al., 2017; Rastak et al., 2017; Altaf et al., 2018).

More recently, researchers have focused on LLPS in SOA particles in the absence of inorganic salts (Peters et al., 2006; Renbaum-Wolff et al., 2016; Rastak et al., 2017; Song et al., 2017; Song et al., 2018) since it is important to explore the CCN properties of the particles (Petters et al., 2006; Hodas et al., 2016; Renbaum-Wolff et al., 2016; Ovadnevaite et al., 2017; Rastak et al., 2017; Liu et al., 2018). Renbaum-Wolff et al. (2016) and Song et al. (2017) observed LLPS at a high RH of ~95–100% in SOA particles produced from ozonolysis of α-pinene, β-caryophyllene, and limonene. However, Rastak et al. (2017) and Song et al. (2017) did not observe LLPS in SOA particles produced from photo-oxidation of isoprene and toluene. The occurrence of LLPS in SOA particles free of inorganic salts was related to the average O:C of the organic materials. When the average O:C of the SOA particle is less than ~0.44, LLPS was observed in the SOA particles free of inorganic salts (Renbaum-Wolff et al., 2016; Rastak et al., 2017; Song et al., 2017). Song et al. (2018) studied organic particles consisting of one and two commercially available organic species free of inorganic salts and found that the average O:C of the organic material can be an important parameter to predict LLPS. LLPS was observed in particles containing one organic species at an O:C ratio of ≤ 0.44 and in particles containing two organic species at an O:C ratio of ≤ 0.58. Since still a few systems have been studied so far, more studies are needed to confirm the effect of O:C for LLPS in organic particles.

Herein, we investigated LLPS in SOA particles produced from ozonolysis and photo-oxidation of α-pinene. Moreover, we studied the effects of NH_3 on SOA particles produced from ozonolysis and photo-oxidation of α-pinene on the occurrence of LLPS.

2 Experimental

2.1 Production of SOA particles

Four different types of SOA particles were generated in the flow tube reactor of Kyungpook National University (KNU), Korea: those produced via α-pinene ozonolysis and α-pinene photo-oxidation in the absence of NH_3 (Table 1), and those produced via α-pinene ozonolysis and α-pinene photo-oxidation in the presence of NH_3 (Table 2). The method of SOA particle

generation was described previously by Babar et al. (2017). The flow tube reactor was run at a flow rate of 4.0 L·min^{-1}, with a residence time of 3.63 min at ~10% RH.

α-pinene of 1000 ppb concentration was injected into the flow tube reactor to produce SOA particles via ozonolysis without NH_3. O_3 was produced by passing high purity O_2 through a UV lamp (λ = 185 nm) and was injected into the flow tube reactor at a concentration of 10000 ppb. Table 1 presents the experimental conditions for the ozonolysis.

To produce SOA particles via photo-oxidation in the absence of NH_3, 1000 ppb of α-pinene was injected in the flow tube reactor (Table 1). OH radical was produced by photo-dissociation of O_3 by irradiating O_3 with UV (λ = 254 nm) in the presence of water vapor. The following photochemical reactions take place.

$$O_3 + h\nu \rightarrow O_2 + O \quad (1)$$

$$O + H_2O \rightarrow 2OH \quad (2)$$

In the flow tube reactor, OH concentrations were determined from the photochemical decay of toluene because toluene is well known for its OH reaction rate. The OH reaction rate constant (k_{OH}) of toluene is 5.48 × 10^{-12} molecules cm^{-3} s^{-1} with insignificant reaction rate with O_3 (Atkinson and Aschmann, 1989). OH concentrations were calculated by varying O_3 and RH from 2000 ppb to 8000 ppb and 10% to 60%, respectively. OH concentrations were calculated by first order decay of toluene by reaction with OH radicals (Babar et al., 2017). Assuming an atmospheric OH concentration of 1.5 x 10^6 molecules·cm^{-3}, OH exposures were 8.2 x 10^{10} molecules·cm^{-3}·s and 2.3 x 10^{11} molecules·cm^{-3}·s, corresponding to atmospheric aging time of 0.5 d and 2.5 d, respectively, and the concentrations of O_3 in the reactor were 2000 and 6000 ppb at 10% RH, respectively.

The same method was used for SOA particle generation via ozonolysis and photo-oxidation in the presence of NH_3, the exception being that NH_3 was injected into the flow tube reactor during particle generation. The concentration of NH_3 was 2000 ppb for the ozonolysis and photo-oxidation (Table 2).

The 4 L·min^{-1} mainstream flow of SOA particles at the outlet of the flow tube reactor was diluted by a humidified air stream (RH of 60%) of 7 L·min^{-1}. A diffusion dryer loaded with

silica gel was used at the upstream of Scanning Mobility Particle Sizer (SMPS+C, Grimm, Germany) for the measurement of dry SOA mass concentrations. After dilution, the mass concentrations of the SOA particles were measured to range between ~480 $\mu g \cdot m^{-3}$ and ~880 $\mu g \cdot m^{-3}$ using the SMPS for different experimental conditions as presented in Tables 1 and 2. The sample and sheath flow rates of the SMPS were 0.3 and 3.0 $L \cdot min^{-1}$, respectively. The SOA particles consisting of up to ~5 μm were collected at the outlet of the reactor on a siliconized substrate (siliconized glass slides of 18 mm, Hampton Research, USA). Figure S1 is an example image of collected SOA particles derived from α-pinene ozonolysis (α-pinene O_3 #1 in Table 1) on a hydrophobic substrate at the outlet of the flow tube reactor.

For each experiment, the siliconized glass slide was initially cleaned three times with water and methanol. Then, it was dried by purging N_2 gas. Finally, it was fixed in the Stage D collector plate of a Sioutas cascade impactor (225-370, SKC, USA), operated at 9 $L \cdot min^{-1}$.

2.2 Observation of liquid-liquid phase separation in SOA particles

The observation of LLPS in a particle required particle diameters of 20–80 μm. In order to obtain the appropriate particle sizes for the LLPS experiments, SOA particles sized up to 5 μm collected on the siliconized substrate from the flow tube reactor were placed into a RH-controlled flow-cell coupled to an optical microscope (Olympus BX43, 40× objective) (Parsons et al., 2004; Pant et al., 2006; Bertram et al., 2011; Song et al., 2012b; Song et al., 2018) at ~100% RH, and then, the particles grew and coagulated for ~60 min. This process resulted in a particle size of 20–80 μm (Renbaum-Wolff et al., 2016). Once the particle size was appropriate for the LLPS experiments, humidity cycles were performed.
During a humidity cycle, RH was reduced from ~100% to ~5 – 10% lower than the RH at which the two liquid phases merged into one phase, followed by an increase to ~100% RH at a rate of 0.1 – 0.5% $RH \cdot min^{-1}$. If LLPS was not observed, RH was reduced from ~100% to ~0%, and then, it was increased to ~100% at a rate of 0.5 – 1.0% $RH \cdot min^{-1}$. We did not observe a dependence of LLPS on the humidity ramp rate. The optical images of the SOA particles during the experiment were recorded every 5 s using a complementary metal oxide semiconductor detector (Digiretina 16, Tucsen, China). All the experiments were performed at a temperature of 289±0.2 K.

The RH was controlled by the ratio of N_2/H_2O gas at a total flow rate of 500 sccm. The RH

inside the flow-cell was determined using a temperature and humidity sensor (Sensirion SHT 71, Switzerland) which was calibrated by observing the deliquescence RH for the following pure inorganic salts at 293 K: potassium carbonate (44% RH), sodium chloride (76% RH), ammonium sulfate (80.5% RH), and potassium nitrate particle (93.5% RH) (Winston and Bates, 1960). The uncertainty of the RH after calibration was ±2.0%.

3 Results and Discussion

3.1 SOA particles produced from α-pinene ozonolysis and α-pinene photo-oxidation

SOA particles generated by α-pinene ozonolysis with a mass concentration of ~500 - 1000 $\mu g \cdot m^{-3}$ underwent humidity cycles at 289 ± 0.2 K. Figure 1 shows examples of optical images of a SOA particle (α-pinene O_3 #1 in Table 1) produced from α-pinene ozonolysis with increasing RH. Only one phase was observed from 0 to ~96% RH (Fig. 1). At 96.6% RH, LLPS occurred by a mechanism of spinodal decomposition, which distributes many small inclusions (Schlieren) throughout a particle (Ciobanu et al., 2009; Song et al., 2012b). After phase separation, at ~97.0% RH, small droplets grew and coagulated to form inner and outer phases in the particle. As the RH increased further, the SOA particle displayed a core–shell morphology consisting of inner and outer phases. The two liquid phases co-existed up to ~100% RH, as shown in Fig. 1. When the RH decreased from ~100%, the inner phase became smaller and merged into one phase at ~95.0% RH. We assume that the inner phase is a water-rich phase and the outer phase is an organic-rich phase since the size of the inner phase depends on changes to RH (Renbaum-Wolff et al., 2016; Song et al., 2017; Song et al., 2018). Moreover, previous studies using surface tension (Jasper, 1972), spreading coefficient (Kwamena et al., 2010; Reid et al., 2011), Raman spectroscopy (Song et al., 2013; Gorkowski et al., 2016; Gorkowski et al., 2017), atomic force microscopy (Zhang et al., 2018), and scanning electron microscopy (O'Brien et al., 2015) showed consistent results with regard to the morphology of the particles consisting of organic and inorganic salts.

Table 1 summarizes the separation relative humidity (SRH) upon moistening and the merging relative humidity (MRH) upon drying. In all cases, the SOA mass concentration was ~500 - 1000 $\mu g \cdot m^{-3}$. LLPS was observed at 95.8 ± 2.3% RH for all SOA particles derived from α-pinene ozonolysis, and the two phases merged into one phase at 92.9 ± 4.6% RH. The

uncertainties of the SRH and the MRH indicate the 2σ from several humidity cycles for one sample and from the uncertainty of the calibration.

Renbaum-Wolff et al. (2016) observed LLPS in SOA particles derived from α-pinene ozonolysis at ~95% RH. It is consistent with our result. They also showed that LLPS in the particles did not depend on SOA particle mass concentrations between 75 and 11000 $\mu g \cdot m^{-3}$. Since the SOA particle mass concentration does not affect LLPS, in this study, we only focused on the SOA particle mass concentration of ~500 - 1000 $\mu g \cdot m^{-3}$ for different types of SOA particles.

We also performed humidity cycles for SOA particles of mass concentration ~500 - 1000 $\mu g \cdot m^{-3}$ derived from α-pinene photo-oxidation. Table 1 summarizes the results of the humidity cycles. None of the SOA particles from α-pinene photo-oxidation underwent LLPS during the RH cycles. Figure 2 shows examples of optical images of a SOA particle (α-pinene OH #2 in Table 1) for increasing RH. From 0 to 100% RH, there was no evidence of occurrence of LLPS in the particles.

3.2 SOA particles produced from α-pinene ozonolysis with NH_3 and α-pinene photo-oxidation with NH_3

Ammonia is an abundant and reactive gaseous species in the atmosphere (Reis et al., 2009; Heald et al., 2012; Reche et al., 2015; Zheng et al., 2015; Sharma et al., 2016; Warner et al., 2016). Previous studies showed that in the presence of NH_3, SOA particles can be formed more effectively (Zhang et al., 2004; Na et al., 2006; Na et al., 2007; Liu et al., 2015a; Liu et al., 2015b; Babar et al., 2017). To investigate the effect of NH_3 on LLPS in SOA particles, we studied LLPS in SOA particles using α-pinene ozonolysis and photo-oxidation in the presence of NH_3. Table 2 presents the experimental conditions for the particle generation. We used the experimental conditions of SOA particle generation via ozonolysis and photo-oxidation (Table 1) in this case too, but we injected 2000 ppb of NH_3 into the flow tube reactor during particle generation (Table 2).

We performed humidity cycles for the SOA particles produced from α-pinene ozonolysis in the presence of NH_3 for the mass concentration of ~500 - 1000 $\mu g \cdot m^{-3}$. Figure 3 shows examples of the optical images of SOA particles produced by α-pinene ozonolysis in the presence of NH_3

as a function of increasing RH (α-pinene O_3/NH_3 #1 in Table 2). Upon moistening, only one phase was present (Fig. 3). As RH increased, the one phase of the SOA particle was separated into two phases at 95.3% RH, the underlying mechanism being spinodal decomposition. At 95.6% RH, small inclusions in the particle coagulated and grew, and then, as RH increased further, a core–shell morphology, with a shell consisting of an organic-rich phase and the core consisting of a water-rich phase on a substrate, were observed. The two liquid phases co-existed up to ~100% RH. When the RH decreased from ~100% RH, the inner phase of the particle became smaller, and eventually, the inner phase merged into one phase at 94.4% RH.

Table 2 summarizes the results of average SRH and MRH during the humidity cycles for the SOA particles produced by α-pinene ozonolysis in the presence of NH_3. LLPS occurred at 95.4 ± 2.9% RH, and the two phases merged into one phase at 94.4 ± 2.7% RH for the all particles (Table 2).

For SOA particles derived from α-pinene photo-oxidation in the presence of NH_3, no LLPS was observed during changes to RH. Table 2 lists the results of SRH and MRH for two different SOA particles derived from α-pinene photo-oxidation in the presence of NH_3. Figure 4 show the examples of the optical images of SOA particles produced by α-pinene with NH_3 photo-oxidation for increasing RH (α-pinene OH/NH_3 #2 in Table 2). Only one phase was observed from 0 to 100% RH.

3.3 Phases of the four different types of SOA particles

Figure 5 shows the RH at which two liquid phases were observed during RH scanning for the four different types of SOA particles. Circles represent MRH upon drying, and triangles represent SRH upon moistening. In the figure, the values of SRH and MRH of SOA particles derived from α-pinene ozonolysis by Renbaum-Wolff et al. (2016) are also included (in red). If RH equals 0%, no LLPS was observed.

Among the four different types of SOA particles, two types of particles underwent LLPS but the remaining particles did not (Fig. 5). For the SOA particles derived from α-pinene ozonolysis, two liquid phases existed at ~95.8 ± 2.3% RH up to ~100 ± 2.0% RH with increasing RH. For values lower than ~92.9 ± 4.6% RH with decreasing RH, only one phase was observed. For the SOA particles derived from α-pinene ozonolysis in the presence of NH_3, the RH range for the

two liquid phases was ~95.4 ± 2.9% and ~100 ± 2.0% with increasing RH. SRH values of both SOA particles were very similar within the uncertainties of the measurements. Also, Fig. 5 showed that the values of SRH upon moistening and MRH upon drying for the two types of particles were close within the uncertainties of the measurements, suggesting that the kinetic barrier to LLPS in the particles is low. Compared to the SOA particles derived from α-pinene ozonolysis and from α-pinene ozonolysis with NH_3, LLPS was not observed in SOA particles derived from α-pinene photo-oxidation without/with NH_3 (Fig. 5). In these cases, only one phase was present between 0 and 100% RH.

3.4 Relation between O:C ratio and LLPS

Recent studies have shown that occurrence of LLPS in SOA particles free of inorganic salts is related to the average O:C ratio of the organic materials (Renbaum-Wolff et al., 2016; Rastak et al., 2017; Song et al., 2017). They showed that LLPS can occur in SOA particles derived from α-pinene, limonene, and β-caryophyllene for RH between ~95% and ~100% when the average O:C ratio ranged from 0.34 and 0.44. LLPS was not observed in SOA particles derived from isoprene and toluene when the average O:C ratio was between 0.52 and 1.30. Figure 6 and Table S1 show LLPS as a function of the average O:C ratio of SOA particles from previous studies (Lambe et al., 2015; Li et al., 2015; Renbaum-Wolff et al., 2016; Song et al., 2017). Also presented in Table S2 are the O:C ratios and experimental conditions for the SOA particles produced from α-pinene ozonolysis and photo-oxidation investigated in this study and previous studies. In this study, data on the average O:C ratios were not available, and thus, we chose the O:C ratios in the literature that were closest to the experimental conditions (Table S2). The O:C ratio for the SOA particles derived from α-pinene ozonolysis ranges from 0.42–0.44 as per Li et al. (2015), whereas that for SOA particles derived from α-pinene photo-oxidation is 0.40–0.90 according to Lambe et al. (2015).

According to the dataset of average O:C ratios of different types of SOA particles from this study as well as previous studies, Fig. 6 shows that LLPS occurred when the average O:C ratio was between 0.34 and 0.44. This range of the O:C ratio required for occurrence of LLPS in the SOA particles is consistent with that of previous work (Renbaum-Wolff et al., 2016; Rastak et al., 2017; Song et al., 2017). However, LLPS did not occur when the average O:C ratio was between 0.45 and 1.30 in this study. Using a new type of SOA particle generated from α-pinene

photo-oxidation, we suggest that the absence of LLPS is wider than that reported by a previous work (0.52 - 1.30) (Song et al., 2017).

Similar to the results of LLPS in the SOA particles with O:C ratio, bulk solutions containing two organics and water also showed the miscibility gap (Ganbavale et al., 2015). For example, bulk solutions of two organics with a low O:C and water (e.g. a mixture of 1-butanol, 1-propanol, and water) formed two liquid phases (Ganbavale et al., 2015). However, bulk solutions of two organics with a high O:C and water (e.g. a mixture of ethanol, acetic acid, and water) formed a single liquid phase.

Previous studies found nitrogen-containing SOA species in the presence of NH_3 (Laskin et al., 2015; Liu et al., 2015b). They suggested that ammonium carboxylates were formed by neutralization between carboxylic acid and ammonia, and amines were formed by carbonyl and ammonia via Schiff's base reaction (Na et al., 2006; Na et al., 2007; Laskin et al., 2015). The nitrogen to carbon (N:C) ratio was reported to be 0.01–0.08 based on aerosol mass spectrometry (AMS) and fourier transform ion cyclotron resonance (FT-ICR MS) (Laskin et al., 2014; Liu et al., 2015b). It is noteworthy that ammonium carboxylates and amines are highly water soluble compounds. However, more accurate data for O:C ratios of the SOA particles in the presence of NH_3 is needed.

Figure 6 also showed the range of the two liquid phases. The two phases consisting of an organic-rich shell and water-rich core were observed at RH as high as ~100% in all cases. Recent studies of Rastak et al. (2017) and Liu et al. (2018) showed from laboratory study and modeling results that the presence of LLPS in organic particles at ~100% RH can lead to lower surface tension, and finally a lower kinetic barrier to CCN activation. Our result can also give an additional insight into attempting more accurate predictions of the CCN properties of organic particles (Petters et al. 2006; Hodas et al. 2016; Renbaum-Wolff et al., 2016; Ovadnevaite et al., 2017; Rastak et al., 2017; Liu et al., 2018).

4 Summary

In this study, we investigated liquid-liquid phase separation of SOA produced from both α-pinene ozonolysis and α-pinene photo-oxidation in the presence or absence of NH_3. We

conducted humidity cycles at a temperature of 289 ± 0.2 K for four different SOA particles derived from α-pinene ozonolysis, α-pinene photo-oxidation, α-pinene ozonolysis with NH_3, and α-pinene photo-oxidation with NH_3, for particle mass concentrations of ~500 - 1000 $\mu g \cdot m^{-3}$. Among the four different types of SOA particles, LLPS occurred in SOA particles produced from α-pinene ozonolysis at 95.8 ± 2.3% RH with increasing RH and in those produced from α-pinene ozonolysis with NH_3 at 95.4 ± 2.9% RH with increasing RH. In both types of particles, the two liquid phases co-existed up to ~100% RH. However, LLPS was not observed in SOA particles produced from α-pinene photo-oxidation and α-pinene photo-oxidation with NH_3. LLPS occurred in the SOA particles produced by α-pinene ozonolysis while no LLPS was observed in the SOA particles produced by α-pinene photo-oxidation. In addition, the occurrence of LLPS did not depend on the presence and absence of NH_3. Analysis of the dataset of average O:C ratios of different types of SOA particles from this study and previous studies indicated that LLPS occurred when the O:C ratio was less than ~0.44, and LLPS did not occur when the O:C ratio was greater than ~0.40.

Considering the range of the O:C ratio of organic particles in the atmosphere (0.2–1.0), these results provide additional evidence that LLPS can occur in organic particles even without the presence of inorganic salts in the atmosphere. Moreover, LLPS occurred in the SOA particles at high RH (as high as ~100%), implying that these results can provide additional information toward the CCN properties of organic particles. Additional studies are needed to confirm LLPS in SOA particles produced using more atmospherically relevant VOC mass concentrations, particle mass concentrations, and submicron sizes.

Author contribution

M.S. and H.J.L. conceived and designed the experiments. S.H., J.B.L., and Z.B.B. performed the experiments and analyzed the data. S.H. and M.S. wrote the manuscript and J.B.L. and H.J.L. edited the manuscript.

Acknowledgement

This work was supported by the National Research Foundation of Korea grant funded by the

Korea Government (MSIP) (2016R1C1B1009243). This research was supported by the National Strategic Project-Fine Particle of the National Research Foundation of Korea (NRF) funded by the Ministry of Science and ICT (MSIT), the Ministry of Environment (ME), and the Ministry of Health and Welfare (MOHW) (2017M3D8A1092015).

References

Altaf, M. B., Dutcher, D. D., Raymond, T. M., Freedman, M. A.: Effect of particle morphology on cloud condensation nuclei activity, ACS. Earth. Space. Chem., 2, 634-639, 10.1021/acsearthspacechem.7b00146, 2018.

Atkinson, R. and Aschmann, S. M.: Rate constants for the gas-phase reactions of the OH radical with a series of aromatic hydrocarbons at 296 ± 2 K, Int. J. Chem. Kinet., 21(5), 355–365, doi:10.1002/kin.550210506, 1989.

Ault, A. P., Guasco, T. L., Ryder, O. S., Baltrusaitis, J., Cuadra-Rodriguez, L. A., Collins, D. B., Ruppel, M. J., Prather, K. A., Bertram, T. H., Grassia, V. H.: Inside versus Outside: Ion Redistribution in HNO3 Reacted Sea Spray Aerosol Particles as Determined by Single Particle Analysis, J. Am. Chem. Soc., 135(39), 14528-14531, 2013.

Babar, Z. B., Park, J.-H., and Lim, H.-J.: Influence of NH_3 on secondary organic aerosols from the ozonolysis and photooxidation of α-pinene in a flow reactor, Atmos. Environ., 164, 71-84, 10.1016/j.atmosenv.2017.05.034, 2017.

Baltensperger, U., Dommen, J., Alfarra, R., Duplissy, J., Gaeggeler, K., Metzger, A., Facchini, M. C., Decesari, S., Finessi, E., Reinnig, C., Schott, M., Warnke, J., Hoffmann, T., Klatzer, B., Puxbaum, H., Geiser, M., Savi, M., Lang, D., Kalberer, M., and Geiser, T.: Combined determination of the chemical composition and of health effects of secondary organic aerosols: The POLYSOA project, J. Aerosol Med. Pulm. D, 21, 145–154, https://doi.org/10.1089/jamp.2007.0655, 2008.

Bertram, A. K., Martin, S. T., Hanna, S. J., Smith, M. L., Bodsworth, A., Chen, Q., Kuwata, M., Liu, A., You, Y., and Zorn, S. R.: Predicting the relative humidities of liquid-liquid phase separation, efflorescence, and deliquescence of mixed particles of ammonium sulfate, organic material, and water using the organic-to-sulfate mass ratio of the particle and the oxygen-to-

carbon elemental ratio of the organic component, Atmos. Chem. Phys., 11, 10995-11006, 10.5194/acp-11-10995-2011, 2011.

Bilde, M., and Svenningsson, B.: CCN activation of slightly soluble organics: the importance of small amounts of inorganic salt and particle phase, Tellus. B., 56, 128-134, DOI 10.1111/j.1600-0889.2004.00090, 2004.

Boge, O., Mutzel, A., Iinuma, Y., Yli-Pirila, P., Kahnt, A., Joutsensaari, J., and Herrmann, H.: Gas-phase products and secondary organic aerosol formation from the ozonolysis and photooxidation of myrcene, Atmos. Environ., 79, 553-560, 2013.

Bones, D. L., Henricksen, D. K., Mang, S. A., Gonsior, M., Bateman, A. P., Nguyen, T. B., Cooper, W. J., and Nizkorodov, S. A.: Appearance of strong absorbers and fluorophores in limonene-O-3 secondary organic aerosol due to NH4+-mediated chemical aging over long time scales, J Geophys. Res-Atmos., 115, 2010.

Chen, S., Brune, W. H., Lambe, A. T., Davidovits, P., and Onasch, T. B.: Modeling organic aerosol from the oxidation of α-pinene in a Potential aerosol mass (PAM) chamber, Atmos. Chem. Phys., 13, 5017-5031, 10.5194/acp-13-5017-2013, 2013.

Chhabra, P. S., Flagan, R. C. and Seinfeld, J. H.: Elemental analysis of chamber organic aerosol using an aerodyne high-resolution aerosol mass spectrometer, Atmos. Chem. Phys., 10(9), 4111–4131, doi:10.5194/acp-10-4111-2010, 2010.

Chhabra, P. S., Ng, N. L., Canagaratna, M. R., Corrigan, A. L., Russell, L. M., Worsnop, D. R., Flagan, R. C., and Seinfeld, J. H.: Elemental composition and oxidation of chamber organic aerosol, Atmos. Chem. Phys., 11, 8827–8845, doi:10.5194/acp-11-8827-2011, 2011.

Ciobanu, V. G., Marcolli, C., Krieger, U. K., Weers, U., and Peter, T.: Liquid-liquid phase separation in mixed organic/inorganic aerosol particles, J. Phys. Chem. A., 113, 10966-10978, 10.1021/jp905054d, 2009.

Clark, C. H., Kacarab, M., Nakao, S., Asa-Awuku, A., Sato, K., and Cocker, D. R.: Temperature Effects on Secondary Organic Aerosol (SOA) from the Dark Ozonolysis and Photo-Oxidation of Isoprene, Environ. Sci. Technol., 50, 5564-5571, 2016.Fard, M. M., Krieger, U. K., and Peter, T.: Shortwave radiative impact of liquid-liquid phase separation in brown carbon aerosols, Atmos. Chem. Phys., 18, 13511-13530, 2018.

Fard, M. M., Krieger, U. K., and Peter, T.: Shortwave radiative impact of liquid-liquid phase separation in brown carbon aerosols, Atmos. Chem. Phys., 18, 13511-13530, 2018.

Forster, P., Ramaswamy, V., Artaxo, P., Berntsen, T., Betts, R., Fahey, D.W., Haywood, J., Lean, J., Lowe, D.C., Myhre, G., Nganga, J., Prinn, R., Raga, G., Schulz, M. and Van Dorland, R., Changes in Atmospheric Constituents and in Radiative Forcing, in Climate Change 2007: The Physical Science Basis. Contribution of working Group I to the Fourth Assessment Report of the Intergovernmental Panel on Climate Changes, edited by Solomon, S., Qin, D., Manning, M., Chen, Z., Marquis, M., Averyt, K.B., Tignor, M. and Miller, H.L. (Cambridge University Press, Cambridge, 2007).

Ganbavale, G., Zuend, A., Marcolli, C., and Peter, T.: Improved AIOMFAC model parameterisation of the temperature dependence of activity coefficients for aqueous organic mixtures, Atmos. Chem. Phys., 15, 447-493, 10.5194/acp-15-447-2015, 2015.

Gorkowski, K., Beydoun, H., Aboff, M., Walker, J. S., Reid, J. P., and Sullivan, R. C.: Advanced aerosol optical tweezers chamber design to facilitate phase-separation and equilibration timescale experiments on complex droplets, Aerosol. Sci. Tech., 50, 1327-1341, 10.1080/02786826.2016.1224317, 2016.

Gorkowski, K., Donahue, N. M., and Sullivan, R. C.: Emulsified and Liquid Liquid Phase-Separated States of alpha-Pinene Secondary Organic Aerosol Determined Using Aerosol Optical Tweezers, Environ. Sci. Technol., 51, 12154-12163, 10.1021/acs.est.7b03250, 2017.

Hallquist, M., Wenger, J. C., Baltensperger, U., Rudich, Y., Simpson, D., Claeys, M., Dommen, J., Donahue, N. M., George, C., Goldstein, A. H., Hamilton, J. F., Herrmann, H., Hoffmann, T., Iinuma, Y., Jang, M., Jenkin, M. E., Jimenez, J. L., Kiendler-Scharr, A., Maenhaut, W., McFiggans, G., Mentel, T. F., Monod, A., Prevot, A. S. H., Seinfeld, J. H., Surratt, J. D., Szmigielski, R., and Wildt, J.: The formation, properties and impact of secondary organic aerosol: current and emerging issues, Atmos. Chem. Phys., 9, 5155-5236, 2009.

Heald, C. L., Collett, J. L., Lee, T., Benedict, K. B., Schwandner, F. M., Li, Y., Clarisse, L., Hurtmans, D. R., Van Damme, M., Clerbaux, C., Coheur, P. F., Philip, S., Martin, R. V., and Pye, H. O. T.: Atmospheric ammonia and particulate inorganic nitrogen over the United States, Atmos. Chem. Phys., 12, 10295-10312, 2012.

Heaton, K. J., Dreyfus, M. A., Wang, S., and Johnston, M. V.: Oligomers in the early stage of biogenic secondary organic aerosol formation and growth, Environ. Sci. Technol., 41, 6129-6136, doi:10.1021/es070314n, 2007.

Hodas, N., Zuend, A., Schilling, K., Berkemeier, T., Shiraiwa, M., Flagan, R. C., and Seinfeld, J. H.: Discontinuities in hygroscopic growth below and above water saturation for laboratory surrogates of oligomers in organic atmospheric aerosols, Atmos. Chem. Phys., 16, 12767-12792, 10.5194/acp-16-12767-2016, 2016.

IPCC: Climate Change 2013: The Physical Science Basis. Contribution of Working Group I to the Fifth Assessment Report of the Intergovernmental Panel on Climate Change, edited by: Stocker, T. F., Qin, D., Plattner, G.-K., Tignor, M., Allen, S. K., Boschung, J., Nauels, A., Xia, Y., Bex, V., and Midgley, P. M., Cambridge University Press, Cambridge, UK and NewYork, NY, USA, 1535, 2013.

Jang, Y., Kim, G., and Chiriboga, D. A.: Correlates of sense of control among older Korean-American immigrants: Financial status, physical health constraints, and environmental challenges, Int. J. Aging. Hum. Dev., 63, 173–186, https://doi.org/10.2190/9qmqTg4a-1ldc-Cnrr, 2006.

Järvinen, E., Ignatius, K., Nichman, L., Kristensen, T. B., Fuchs, C., Hoyle, C. R., Höppel, N., Corbin, J. C., Craven, J., Duplissy, J., Ehrhart, S., El Haddad, I., Frege, C., Gordon, H., Jokinen, T., Kallinger, P., Kirkby, J., Kiselev, A., Naumann, K. H., Petäjä, T., Pinterich, T., Prevot, A. S. H., Saathoff, H., Schiebel, T., Sengupta, K., Simon, M., Slowik, J. G., Tröstl, J., Virtanen, A., Vochezer, P., Vogt, S., Wagner, A. C., Wagner, R., Williamson, C., Winkler, P. M., Yan, C., Baltensperger, U., Donahue, N. M., Flagan, R. C., Gallagher, M., Hansel, A., Kulmala, M., Stratmann, F., Worsnop, D. R., Möhler, O., Leisner, T. and Schnaiter, M.: Observation of viscosity transition in α-pinene secondary organic aerosol, Atmos. Chem. Phys., 16(7), 4423–4438, doi:10.5194/acp-16-4423-2016, 2016.

Jasper, J. J.: The surface tension of pure liquid compounds, J. Phys. Chem. Ref. Data, 1, 841–1009, https://doi.org/10.1063/1.3253106, 1972.

Jimenez, J. L., Canagaratna, M. R., Donahue, N. M., Prevot, A. S. H., Zhang, Q., Kroll, J. H., DeCarlo, P. F., Allan, J. D., Coe, H., Ng, N. L., Aiken, A. C., Docherty, K. S., Ulbrich, I. M., Grieshop, A. P., Robinson, A. L., Duplissy, J., Smith, J. D., Wilson, K. R., Lanz, V. A., Hueglin,

C., Sun, Y. L., Tian, J., Laaksonen, A., Raatikainen, T., Rautiainen, J., Vaattovaara, P., Ehn, M., Kulmala, M., Tomlinson, J. M., Collins, D. R., Cubison, M. J., Dunlea, E. J., Huffman, J. A., Onasch, T. B., Alfarra, M. R., Williams, P. I., Bower, K., Kondo, Y., Schneider, J., Drewnick, F., Borrmann, S., Weimer, S., Demerjian, K., Salcedo, D., Cottrell, L., Griffin, R., Takami, A., Miyoshi, T., Hatakeyama, S., Shimono, A., Sun, J. Y., Zhang, Y. M., Dzepina, K., Kimmel, J. R., Sueper, D., Jayne, J. T., Herndon, S. C., Trimborn, A. M., Williams, L. R., Wood, E. C., Middlebrook, A. M., Kolb, C. E., Baltensperger, U., and Worsnop, D. R.: Evolution of Organic Aerosols in the Atmosphere, Science., 326, 1525-1529, 2009.

Kanakidou, M., Seinfeld, J. H., Pandis, S. N., Barnes, I., Dentener, F. J., Facchini, M. C., Van Dingenen, R., Ervens, B., Nenes, A., Nielsen, C. J., Swietlicki, E., Putaud, J. P., Balkanski, Y., Fuzzi, S., Horth, J., Moortgat, G. K., Winterhalter, R., Myhre, C. E. L., Tsigaridis, K., Vignati, E., Stephanou, E. G., and Wilson, J.: Organic aerosol and global climate modelling: a review, Atmos. Chem. Phys., 5, 1053-1123, DOI 10.5194/acp-5-1053-2005, 2005.

Kim, H., Liu, S., Russell, L. M., and Paulson, S. E.: Dependence of Real Refractive Indices on O:C, H:C and Mass Fragments of Secondary Organic Aerosol Generated from Ozonolysis and Photooxidation of Limonene and alpha-Pinene, Aerosol. Sci. Tech., 48, 498-507, 2014.

Knopf, D. A., Alpert, P. A., and Wang, B. B.: The Role of Organic Aerosol in Atmospheric Ice Nucleation: A Review, ACS. Earth. Space. Chem., 2, 168-202, 10.1021/acsearthspacechem.7b00120, 2018.

Krieger, U. K., Marcolli, C., and Reid, J. P.: Exploring the complexity of aerosol particle properties and processes using single particle techniques, Chem. Soc. Rev., 41, 6631-6662, 10.1039/c2cs35082c, 2012.

Kuwata, M., and Martin, S. T.: Phase of atmospheric secondary organic material affects its reactivity., P. Natl. Acad. Sci. USA., 109, 17354-17359, 10.1073/pnas.1209071109, 2012.

Kwamena, N. O. A., Buajarern, J., and Reid, J. P.: Equilibrium Morphology of Mixed Organic/Inorganic/Aqueous Aerosol Droplets: Investigating the Effect of Relative Humidity and Surfactants, J. Phys. Chem. A., 114, 5787-5795, 10.1021/jp1003648, 2010.

Lambe, A. T., Chhabra, P. S., Onasch, T. B., Brune, W. H., Hunter, J. F., Kroll, J. H., Cummings, M. J., Brogan, J. F., Parmar, Y., Worsnop, D. R., Kolb, C. E., and Davidovits, P.: Effect of

oxidant concentration, exposure time, and seed particles on secondary organic aerosol chemical composition and yield, Atmos. Chem. Phys., 15, 3063-3075, 10.5194/acp-15-3063-2015, 2015.

Laskin, J., Laskin, A., Nizkorodov, S. A., Roach, P., Eckert, P., Gilles, M. K., Wang, B. B., Lee, H. J., and Hu, Q. C.: Molecular Selectivity of Brown Carbon Chromophores, Environ. Sci. Technol., 48, 12047-12055, 10.1021/es503432r, 2014.

Laskin, A., Laskin, J., and Nizkorodov, S. A.: Chemistry of Atmospheric Brown Carbon, Chem. Rev., 115, 4335-4382, 10.1021/cr5006167, 2015.

Li, Y. J., Liu, P., Gong, Z., Wang, Y., Bateman, A. P., Bergoend, C., Bertram, A. K., and Martin, S. T.: Chemical Reactivity and Liquid/Nonliquid States of Secondary Organic Material, Environ. Sci. Technol., 49, 13264-13274, 10.1021/acs.est.5b03392, 2015.

Liu, S., Shilling, J. E., Song, C., Hiranuma, N., Zaveri, R. A., and Russell, L. M.: Hydrolysis of Organonitrate Functional Groups in Aerosol Particles, Aerosol. Sci. Tech., 46, 1359-1369, 10.1080/02786826.2012.716175, 2012.

Liu, T. Y., Wang, X. M., Deng, W., Zhang, Y. L., Chu, B. W., Ding, X., Hu, Q. H., He, H., and Hao, J. M.: Role of ammonia in forming secondary aerosols from gasoline vehicle exhaust, Sci. China. Chem., 58, 1377-1384, 10.1007/s11426-015-5414-x, 2015.

Liu, Y., Liggio, J., and Staebler, R.: Reactive uptake of ammonia to secondary organic aerosols: Kinetics of organonitrogen formation, Atmos. Chem. Phys., 15, 13569-13584, 10.5194/acp-15-13569-2015, 2015.

Liu, P. F., Song, M., Zhao, T. N., Gunthe, S. S., Ham, S. H., He, Y. P., Qin, Y. M., Gong, Z. H., Amorim, J. C., Bertram, A. K., and Martin, S. T.: Resolving the mechanisms of hygroscopic growth and cloud condensation nuclei activity for organic particulate matter, Nat. Commun., 9, ARTN 4076 10.1038/s41467-018-06622-2, 2018.

Marcolli, C., and Krieger, U. K.: Phase changes during hygroscopic cycles of mixed organic/inorganic model systems of tropospheric aerosols, J. Phys. Chem. A., 110, 1881-1893, 10.1021/jp0556759, 2006.

Martin, S. T.: Phase transitions of aqueous atmospheric particles, Chem. Rev., 100, 3403-3453, 2000.

Martin, S. T., Hung, H. M., Park, R. J., Jacob, D. J., Spurr, R. J. D., Chance, K. V., and Chin, M.: Effects of the physical state of tropospheric ammonium-sulfate-nitrate particles on global aerosol direct radiative forcing, Atmos. Chem. Phys., 4, 183-214, DOI 10.5194/acp-4-183-2004, 2004.

Massoli, P., Lambe, A. T., Ahern, A. T., Williams, L. R., Ehn, M., Mikkilä, J., Canagaratna, M. R., Brune, W. H., Onasch, T. B., Jayne, J. T., Petäjä, T., Kulmala, M., Laaksonen, A., Kolb, C. E., Davidovits, P., and Worsnop, D. R.: Relationship between aerosol oxidation level and hygroscopic properties of laboratory generated secondary organic aerosol (SOA) particles, Geophys. Res. Lett., 37, 1-5, 10.1029/2010GL045258, 2010.

Murray, B. J., Wilson, T. W., Dobbie, S., Cui, Z. Q., Al-Jumur, S. M. R. K., Mohler, O., Schnaiter, M., Wagner, R., Benz, S., Niemand, M., Saathoff, H., Ebert, V., Wagner, S., and Karcher, B.: Heterogeneous nucleation of ice particles on glassy aerosols under cirrus conditions, Nat. Geosci., 3, 233-237, 10.1038/Ngeo817, 2010.

Na, K., Song, C., and Cocker, D. R.: Formation of secondary organic aerosol from the reaction of styrene with ozone in the presence and absence of ammonia and water, Atmos. Environ., 40, 1889-1900, 10.1016/j.atmosenv.2005.10.063, 2006.

Na, K., Song, C., Switzer, C., and Cocker, D. R.: Effect of ammonia on secondary organic aerosol formation from alpha-Pinene ozonolysis in dry and humid conditions, Environ. Sci. Technol., 41, 6096-6102, 10.1021/es061956y, 2007.

Nguyen, T. B., Laskin, A., Laskin, J., and Nizkorodov, S. A.: Brown carbon formation from ketoaldehydes of biogenic monoterpenes, Faraday. Discuss., 165, 473-494, 2013.

O'Brien, R. E., Wang, B. B., Kelly, S. T., Lundt, N., You, Y., Bertram, A. K., Leone, S. R., Laskin, A., and Gilles, M. K.: Liquid-Liquid Phase Separation in Aerosol Particles: Imaging at the Nanometer Scale, Environ. Sci. Technol., 49, 4995-5002, 10.1021/acs.est.5b00062, 2015.

Ovadnevaite, J., Zuend, A., Laaksonen, A., Sanchez, K. J., Roberts, G., Ceburnis, D., Decesari, S., Rinaldi, M., Hodas, N., Facchini, M. C., Seinfeld, J. H., and Dowd, C. O.: Surface tension prevails over solute effect in organic-influenced cloud droplet activation, Nature, 546, 637-641, 10.1038/nature22806, 2017.

Pajunoja, A., Lambe, A. T., Hakala, J., Rastak, N., Cummings, M. J., Brogan, J. F., Hao, L., Paramonov, M., Hong, J., Prisle, N. L., Malila, J., Romakkaniemi, S., Lehtinen, K. E. J., Laaksonen, A., Kulmala, M., Massoli, P., Onasch, T. B., Donahue, N. M., Riipinen, I., Davidovits, P., Worsnop, D. R., Petäjä, T., and Virtanen, A.: Adsorptive uptake of water by semisolid secondary organic aerosols, Geophys. Res. Lett., 42, 3063-3068, 10.1002/2015GL063142, 2015.

Pankow, J. F.: Gas/particle partitioning of neutral and ionizing compounds to single and multi-phase aerosol particles. 1. Unified modeling framework, Atmos. Environ., 37, 3323-3333, 10.1016/S1352-2310(03)00346-7, 2003.

Pant, A., Parsons, M. T., and Bertram, A. K.: Crystallization of aqueous ammonium sulfate particles internally mixed with soot and kaolinite: Crystallization relative humidities and nucleation rates, J. Phys. Chem. A., 110, 8701-8709, 10.1021/jp060985s, 2006.

Parsons, M. T., Mak, J., Lipetz, S. R., and Bertram, A. K.: Deliquescence of malonic, succinic, glutaric, and adipic acid particles, J. Geophys. Res-Atmos., 109, Artn D06212, 10.1029/2003jd004075, 2004.

Petters, M. D., Kreidenweis, S. M., Snider, J. R., Koehler, K. A., Wang, Q., Prenni, A. J., and Demott, P. J.: Cloud droplet activation of polymerized organic aerosol, Tellus. B., 58, 196-205, 10.1111/j.1600-0889.2006.00181.x, 2006.

Pfaffenberger, L., Barmet, P., Slowik, J. G., Praplan, A. P., Dommen, J., Prévôt, A. S. H., and Baltensperger, U.: The link between organic aerosol mass loading and degree of oxygenation: an α- pinene photooxidation study, Atmos. Chem. Phys., 13, 6493–6506, doi:10.5194/acp-13-6493-2013, 2013.

Poschl, U., and Shiraiwa, M.: Multiphase Chemistry at the Atmosphere-Biosphere Interface Influencing Climate and Public Health in the Anthropocene, Chem. Rev., 115, 4440-4475, 10.1021/cr500487s, 2015.

Rastak, N., Pajunoja, A., Navarro, J. C. A., Ma, J., Song, M., Partridge, D. G., Kirkevag, A., Leong, Y., Hu, W. W., Taylor, N. F., Lambe, A., Cerully, K., Bougiatioti, A., Liu, P., Krejci, R., Petaja, T., Percival, C., Davidovits, P., Worsnop, D. R., Ekman, A. M. L., Nenes, A., Martin, S., Jimenez, J. L., Collins, D. R., Topping, D. O., Bertram, A. K., Zuend, A., Virtanen, A., and

Riipinen, I.: Microphysical explanation of the RH-dependent water affinity of biogenic organic aerosol and its importance for climate, Geophys. Res. Lett., 44, 5167-5177, 2017.

Raymond, T. M., and Pandis, S. N.: Cloud activation of single-component organic aerosol particles, J. Geophys. Res-Atmos., 107, Artn 4787, 10.1029/2002jd002159, 2002.

Reche, C., Viana, M., Karanasiou, A., Cusack, M., Alastuey, A., Artinano, B., Revuelta, M. A., Lopez-Mahia, P., Blanco-Heras, G., Rodriguez, S., de la Campa, A. M. S., Fernandez-Camacho, R., Gonzalez-Castanedo, Y., Mantilla, E., Tang, Y. S., and Querol, X.: Urban NH3 levels and sources in six major Spanish cities, Chemosphere., 119, 769-777, 10.1016/j.chemosphere.2014.07.097, 2015.

Reid, J. P., Dennis-Smither, B. J., Kwamena, N. O. A., Miles, R. E. H., Hanford, K. L., and Homer, C. J.: The morphology of aerosol particles consisting of hydrophobic and hydrophilic phases: hydrocarbons, alcohols and fatty acids as the hydrophobic component, Phys. Chem. Chem. Phys., 13, 15559-15572, 10.1039/c1cp21510h, 2011.

Reis, S., Pinder, R. W., Zhang, M., Lijie, G., and Sutton, M. A.: Reactive nitrogen in atmospheric emission inventories, Atmos. Chem. Phys., 9, 7657-7677, 2009.

Renbaum-wolff, L., Song, M., Marcolli, C., Zhang, Y., and Liu, P. F.: Observations and implications of liquid – liquid phase separation at high relative humidities in secondary organic material produced by α -pinene ozonolysis without inorganic salts, Atmos. Chem. Phys., 16, 7969-7979, 10.5194/acp-16-7969-2016, 2016.Sharma, S. K., Rohtash, Mandal, T. K., Deb, N. C., and Pal, S.: Measurement of Ambient NH3, NO and NO2 at an Urban Area of Kolkata, India, Mapan-J. Metrol. Soc. I., 31, 75-80, 10.1007/s12647-015-0147-z, 2016.

Sharma, S. K., Rohtash, Mandal, T. K., Deb, N. C., and Pal, S.: Measurement of Ambient NH3, NO and NO2 at an Urban Area of Kolkata, India, Mapan-J. Metrol. Soc. I., 31, 75-80, 10.1007/s12647-015-0147-z, 2016.

Shilling, J. E., Chen, Q., King, S. M., Rosenoern, T., Kroll, J. H., Worsnop, D. R., DeCarlo, P. F., Aiken, A. C., Sueper, D., Jimenez, J. L., Martin, S. T.: Loading-dependent elemental composition of α-pinene SOA particles, Atmos. Chem. Phys., 9, 771-782, 10.5194/acp-9-771-2009, 2009.

Shiraiwa, M., Zuend, A., Bertram, A. K., and Seinfeld, J. H.: Gas-particle partitioning of atmospheric aerosols: interplay of physical state, non-ideal mixing and morphology, Phys. Chem. Chem. Phys., 15, 11441-11453, 10.1039/c3cp51595h, 2013.

Shiraiwa, M., Ueda, K., Pozzer, A., Lammel, G., Kampf, C. J., Fushimi, A., Enami, S., Arangio, A. M., Frohlich-Nowoisky, J., Fujitani, Y., Furuyama, A., Lakey, P. S. J., Lelieveld, J., Lucas, K., Morino, Y., Poschl, U., Takaharna, S., Takami, A., Tong, H. J., Weber, B., Yoshino, A., and Sato, K.: Aerosol Health Effects from Molecular to Global Scales, Environ. Sci. Technol., 51, 13545-13567, 10.1021/acs.est.7b04417, 2017.

Song, M., Marcolli, C., Krieger, U. K., Zuend, A., and Peter, T.: Liquid-liquid phase separation in aerosol particles: Dependence on O:C, organic functionalities, and compositional complexity, Geophys. Res. Lett., 39, 1-5, 10.1029/2012GL052807, 2012.

Song, M., Marcolli, C., Krieger, U. K., Zuend, A., and Peter, T.: Liquid-liquid phase separation and morphology of internally mixed dicarboxylic acids/ammonium sulfate/water particles, Atmos. Chem. Phys., 12, 2691-2712, 10.5194/acp-12-2691-2012, 2012.

Song, M., Marcolli, C., Krieger, U. K., Lienhard, D. M., and Peter, T.: Morphologies of mixed organic/inorganic/aqueous aerosol droplets, Faraday. Discuss., 165, 289-316, 10.1039/c3fd00049d, 2013.

Song, M., Liu, P. F., Hanna, S. J., Li, Y. J., Martin, S. T., and Bertram, A. K.: Relative humidity-dependent viscosities of isoprene-derived secondary organic material and atmospheric implications for isoprene-dominant forests, Atmos. Chem. Phys., 15, 5145-5159, 10.5194/acp-15-5145-2015, 2015.

Song, M., Liu, P. F., Martin, S. T., and Bertram, A. K.: Liquid-liquid phase separation in particles containing secondary organic material free of inorganic salts, Atmos. Chem. Phys., 17, 11261-11271, 2017.

Song, M., Ham, S. H., Andrews, R. J., You, Y., Bertram, A. K.: Liquid-liquid phase separation in organic particles containing one and two organic species: importance of the average O:C, Atmos. Chem. Phys., 18, 1680-7375, 10.5194/acp-2018-421, 2018.

Stirnweis, L., Marcolli, C., Dommen, J., Barmet, P., Frege, C., Platt, S. M., Bruns, E. A., Krapf,

M., Slowik, J. G., Wolf, R., Prévôt, A. S. H., Baltensperger, U., and El-Haddad, I.: Assessing the influence of NO_x concentrations and relative humidity on secondary organic aerosol yields from α-pinene photo-oxidation through smog, Atmos. Chem. Phys., 17, 5035-5061, 10.5194/acp-17-5035-2017, 2017.

Stoicescu, C., Iulian, O., and Isopescu, R.: Liquid-Liquid Phase Equilibria of 1-Propanol + Water plus n-Alcohol Ternary Systems at 298.15 K and Atmospheric Pressure, J. Chem. Eng. Data., 56, 3214-3221, 2011.

Tuet, W. Y., Chen, Y., Xu, L., Fok, S., Gao, D., Weber, R. J., and Ng, N. L.: Chemical oxidative potential of secondary organic aerosol (SOA) generated from the photooxidation of biogenic and anthropogenic volatile organic compounds, Atmos. Chem. Phys., 17, 839-853, 10.5194/acp-17-839-2017, 2017.

Updyke, K. M., Nguyen, T. B., and Nizkorodov, S. A.: Formation of brown carbon via reactions of ammonia with secondary organic aerosols from biogenic and anthropogenic precursors, Atmos. Environ., 63, 22-31, 2012.

Veghte, D. P., Altaf, M. B., and Freedman, M. A.: Size Dependence of the Structure of Organic Aerosol, J. Am. Chem. Soc., 135, 16046-16049, 10.1021/ja408903g, 2013.

Wang, B. B., Lambe, A. T., Massoli, P., Onasch, T. B., Davidovits, P., Worsnop, D. R., and Knopf, D. A.: The deposition ice nucleation and immersion freezing potential of amorphous secondary organic aerosol: Pathways for ice and mixed-phase cloud formation, J. Geophys. Res-Atmos., 117, Artn D16209 10.1029/2012jd018063, 2012.

Warner, J. X., Wei, Z. G., Strow, L. L., Dickerson, R. R., and Nowak, J. B.: The global tropospheric ammonia distribution as seen in the 13-year AIRS measurement record, Atmos. Chem. Phys., 16, 5467-5479, 10.5194/acp-16-5467-2016, 2016.

Winston, P. W. and Bates, D. H.: Saturated Solutions for the Control of Humidity in Biological-Research, Ecology, 41, 232–237, https://doi.org/10.2307/1931961, 1960.

You, Y., Renbaum-Wolff, L., and Bertram, A. K.: Liquid-liquid phase separation in particles containing organics mixed with ammonium sulfate, ammonium bisulfate, ammonium nitrate or sodium chloride, Atmos. Chem. Phys., 13, 11723-11734, 10.5194/acp-13-11723-2013, 2013.

You, Y., Smith, M. L., Song, M., Martin, S. T., and Bertram, A. K.: Liquid–liquid phase separation in atmospherically relevant particles consisting of organic species and inorganic salts, Int. Rev. Phys. Chem., 33, 43-77, 10.1080/0144235X.2014.890786, 2014.

Zhang, R. Y., Suh, I., Zhao, J., Zhang, D., Fortner, E. C., Tie, X. X., Molina, L. T., and Molina, M. J.: Atmospheric new particle formation enhanced by organic acids, Science., 304, 1487-1490, DOI 10.1126/science.1095139, 2004.

Zhang, Q., Jimenez, J. L., Canagaratna, M. R., Allan, J. D., Coe, H., Ulbrich, I., Alfarra, M. R., Takami, A., Middlebrook, A. M., Sun, Y. L., Dzepina, K., Dunlea, E., Docherty, K., DeCarlo, P. F., Salcedo, D., Onasch, T., Jayne, J. T., Miyoshi, T., Shimono, A., Hatakeyama, S., Takegawa, N., Kondo, Y., Schneider, J., Drewnick, F., Borrmann, S., Weimer, S., Demerjian, K., Williams, P., Bower, K., Bahreini, R., Cottrell, L., Griffin, R. J., Rautiainen, J., Sun, J. Y., Zhang, Y. M., and Worsnop, D. R.: Ubiquity and dominance of oxygenated species in organic aerosols in anthropogenically-influenced Northern Hemisphere midlatitudes, Geophys. Res. Lett., 34, 2007.

Zhang, X., McVay, R. C., Huang, D. D., Dalleska, N. F., Aumont, B., Flagan, R. C. and Seinfeld, J. H.: Formation and evolution of molecular products in α-pinene secondary organic aerosol, P. Natl. Acad. Sci., 112(46), 14168–14173, doi:10.1073/pnas.1517742112, 2015b.

Zhang, Y., Sanchez, M. S., Douet, C., Wang, Y., Bateman, A. P., Gong, Z., Kuwata, M., Renbaum-Wolff, L., Sato, B. B., Liu, P. F., Bertram, A. K., Geiger, F. M., and Martin S. T.: Changing shapes and implied viscosities of suspended submicron particles, Atmos. Chem. Phys., 15, 7819-7829, 10.5194/acp-15-7819-2015, 2015a.

Zhang, Y., Chen, Y. Z., Lambe, A. T., Olson, N. E., Lei, Z. Y., Craig, R. L., Zhang, Z. F., Gold, A., Onasch, T. B., Jayne, J. T., Worsnop, D. R., Gaston, C. J., Thornton, J. A., Vizuete, W., Ault, A. P., and Surratt, J. D.: Effect of the Aerosol-Phase State on Secondary Organic Aerosol Formation from the Reactive Uptake of Isoprene-Derived Epoxydiols (IEPDX), Environ. Sci. Tech. Let., 5, 167-174, 10.1021/acs.estlett.8b00044, 2018.

Zhao, D., Schmitt, S. H., Wang, M., Acir, I.-H., Tillmann, R., Tan, Z., Novelli, A., Fuchs, H., Pullinen, I., Wegener, R., Rohrer, F., Wildt, J., Kiendler-Scharr, A., Wahner, A., and Mentel, T. F.: Effects of NO_x and SO_2 on the Secondary Organic Aerosol Formation from Photooxidation

of α-pinene and Limonene, Atmos. Chem. Phys. Discuss.., 1-26, 10.5194/acp-2017-294, 2017.

Zuend, A., Marcolli, C., Peter, T., and Seinfeld, J. H.: Computation of liquid-liquid equilibria and phase stabilities: implications for RH-dependent gas/particle partitioning of organic-inorganic aerosols, Atmos. Chem. Phys., 10, 7795-7820, 10.5194/acp-10-7795-2010, 2010.

Zuend, A., and Seinfeld, J. H.: Modeling the gas-particle partitioning of secondary organic aerosol: the importance of liquid-liquid phase separation, Atmos. Chem. Phys., 12, 3857-3882, 10.5194/acp-12-3857-2012, 2012.

Zheng, J., Ma, Y., Chen, M. D., Zhang, Q., Wang, L., Khalizov, A. F., Yao, L., Wang, Z., Wang, X., and Chen, L. X.: Measurement of atmospheric amines and ammonia using the high resolution time-of-flight chemical ionization mass spectrometry, Atmos. Environ., 102, 249-259, 10.1016/j.atmosenv.2014.12.002, 2015.

Table 1. Experimental conditions for production and collection of SOA particles from α-pinene ozone (termed 'α-pinene O_3') and photo-oxidation (termed 'α-pinene OH'). The separation relative humidity (SRH) upon moistening and the merging relative humidity (MRH) upon drying are listed. The SRH is the RH at which liquid-liquid phase separation occurred. The MRH is the RH at which two phases merged into one phase. The uncertainties indicate the 2σ from several humidity cycles for one sample and from the uncertainty of the calibration. SRH = 0 and MRH = 0 indicate that phase separation was not observed.

SOA sample	α-pinene conc. (ppb)	OH exposure (day)	O_3 conc. (ppb)	NH_3 conc. (ppb)	[a]Mass conc. ($\mu g\ m^{-3}$)	[a]Geomean diameter (nm)	SRH (%)	MRH (%)
α-pinene O_3 #1	1000	-	10000	0	481	63	96.0 ± 2.3	94.3 ± 3.1
α-pinene O_3 #2	1000	-	10000	0	493	63	95.4 ± 2.0	91.6 ± 4.4
α-pinene OH #1	1000	0.5	2000	0	688	67	0	0
α-pinene OH #2	1000	2.5	6000	0	479	67	0	0
α-pinene OH #3	1000	0.5	2000	0	633	67	0	0
α-pinene OH #4	1000	2.5	6000	0	618	66	0	0

[a]After dilution of 4 L min^{-1} mainstream with 7 L min^{-1} of humidified air at 60% RH

Table 2. Experimental conditions for production and collection of SOA particles from α-pinene ozone with NH_3 (termed 'α-pinene O_3/NH_3') and photo-oxidation with NH_3 (termed 'α-pinene OH/NH_3'). The separation relative humidity (SRH) upon moistening and the merging relative humidity (MRH) upon drying are listed. The SRH is the RH at which liquid-liquid phase separation occurred. The MRH is the RH at which two phases merged into one phase. The uncertainties indicate the 2σ from several humidity cycles for one sample and from the uncertainty of the calibration. SRH = 0 and MRH = 0 indicate that LLPS was not observed.

SOA sample	α-pinene conc. (ppb)	OH exposure (day)	O_3 conc. (ppb)	NH_3 conc. (ppb)	[a]Mass conc. ($\mu g\ m^{-3}$)	[a]Geomean diameter (nm)	SRH (%)	MRH (%)
α-pinene O_3/NH_3 #1	1000	-	10000	2000	564	68	95.4 ± 3.0	94.0 ± 2.6
α-pinene O_3/NH_3 #2	1000	-	10000	2000	579	68	95.4 ± 3.4	95.1 ± 2.1
α-pinene OH/NH_3 #1	1000	2.5	6000	2000	753	73	0	0
α-pinene OH/NH_3 #2	1000	0.5	2000	2000	886	74	0	0

[a]After dilution of 4 L min^{-1} mainstream with 7 L min^{-1} of humidified air at 60% RH

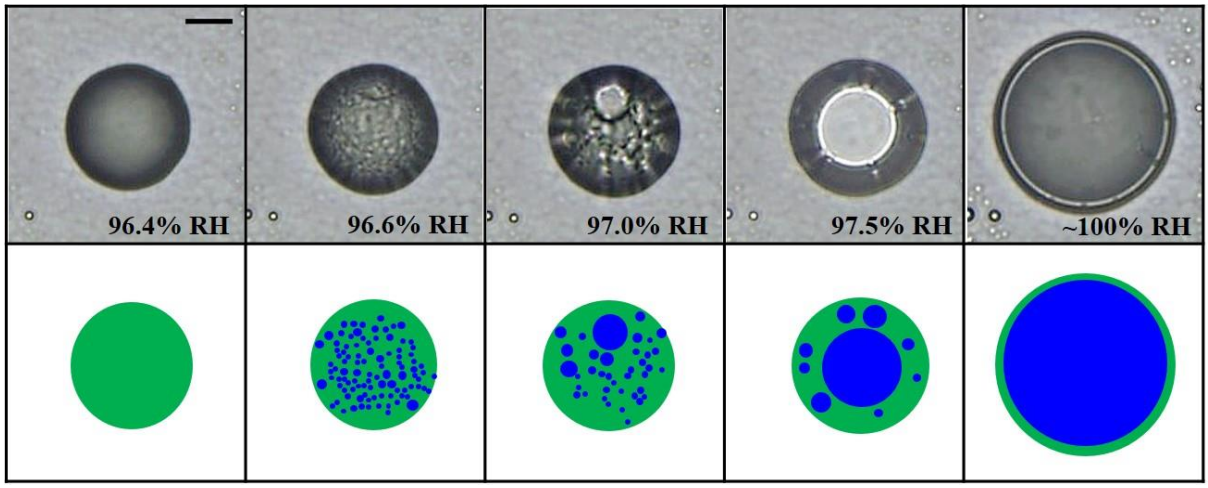

Figure 1. Optical images of a SOA particle produced from α-pinene ozonolysis (α-pinene O_3 #1 in Table 1) with increasing RH. Illustrations is for clarifying the image. Green is SOA rich phase, and blue is water rich phase. Scale bar is 20 μm.

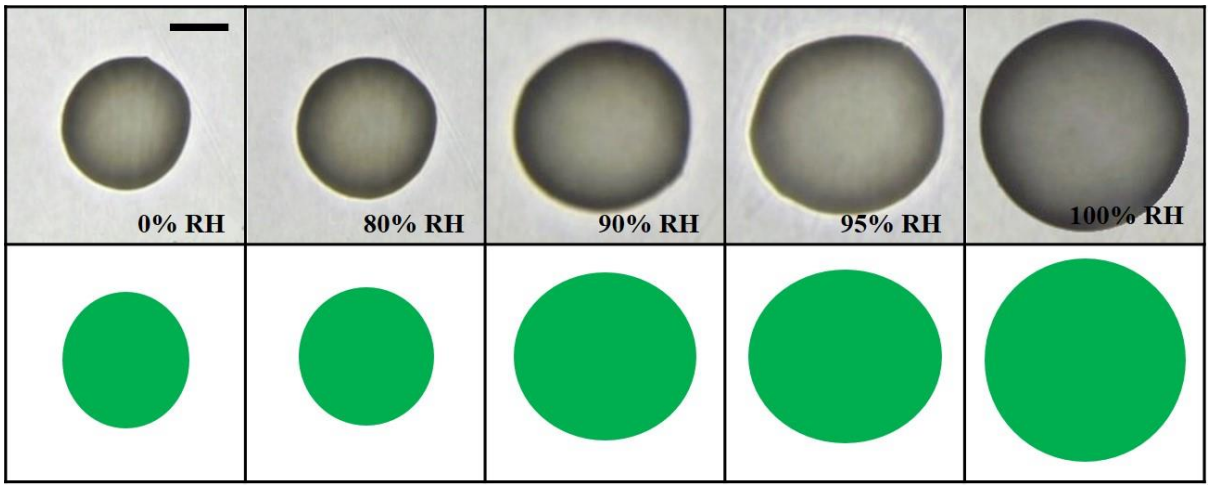

Figure 2. Optical images of a SOA particle produced from α-pinene photo-oxidation (α-pinene OH #2 in Table 1) with increasing RH. Illustrations is for clarifying the image. Green is SOA rich phase, and blue is water rich phase. Scale bar is 20 μm.

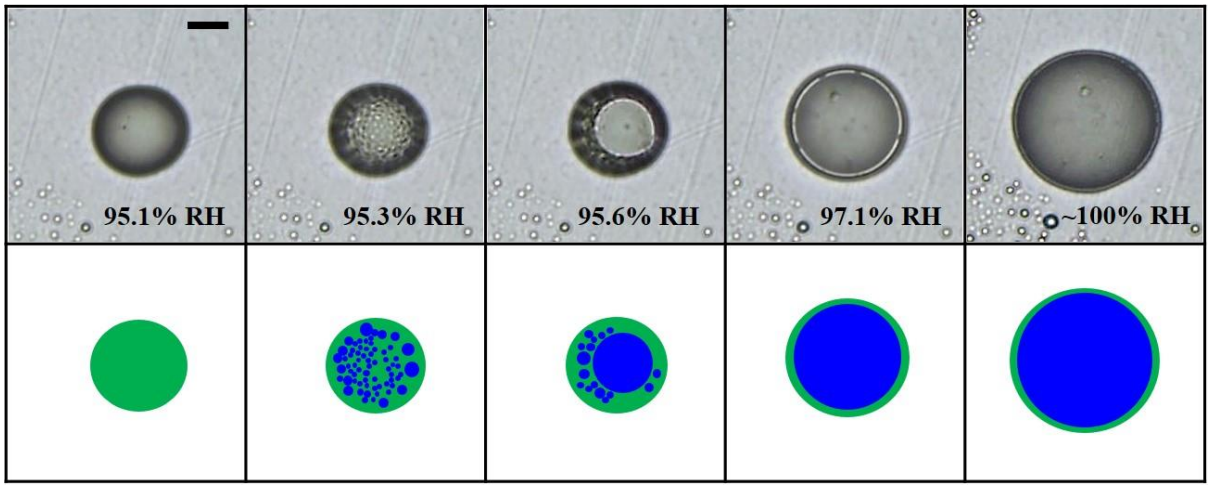

Figure 3. Optical images of a SOA particle produced from α-pinene ozonolysis with NH_3 (α-pinene O_3/NH_3 #1 in Table 2) with increasing RH. Illustrations is for clarifying the image. Green is SOA rich phase, and blue is water rich phase. Scale bar is 20 μm.

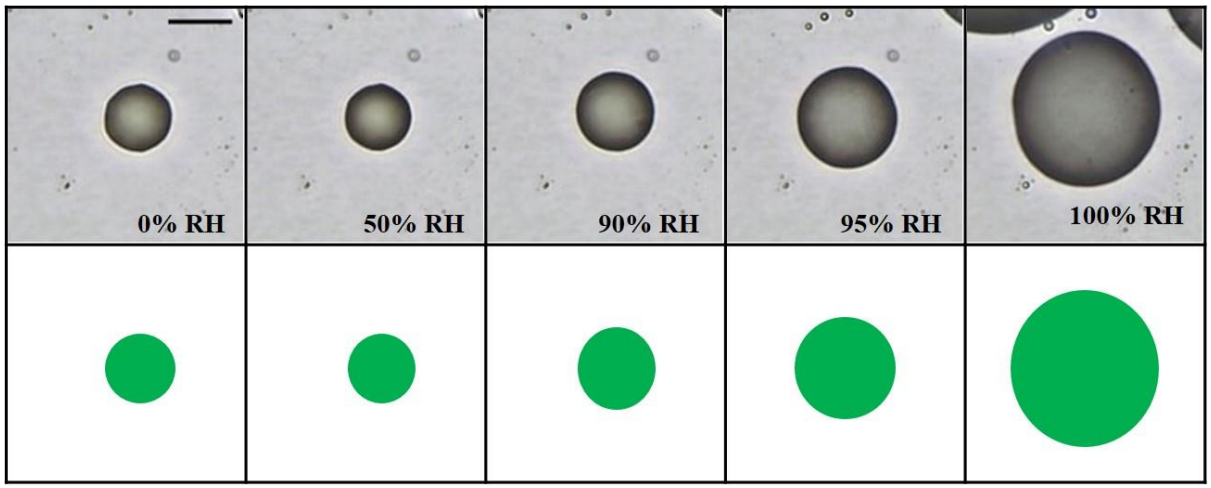

Figure 4. Optical images of a SOA particle produced from α-pinene photo-oxidation with NH_3 (α-pinene OH/NH_3 #2 in Table 1) with increasing RH. Illustrations is for clarifying the image. Green is SOA rich phase, and blue is water rich phase. Scale bar is 20 μm.

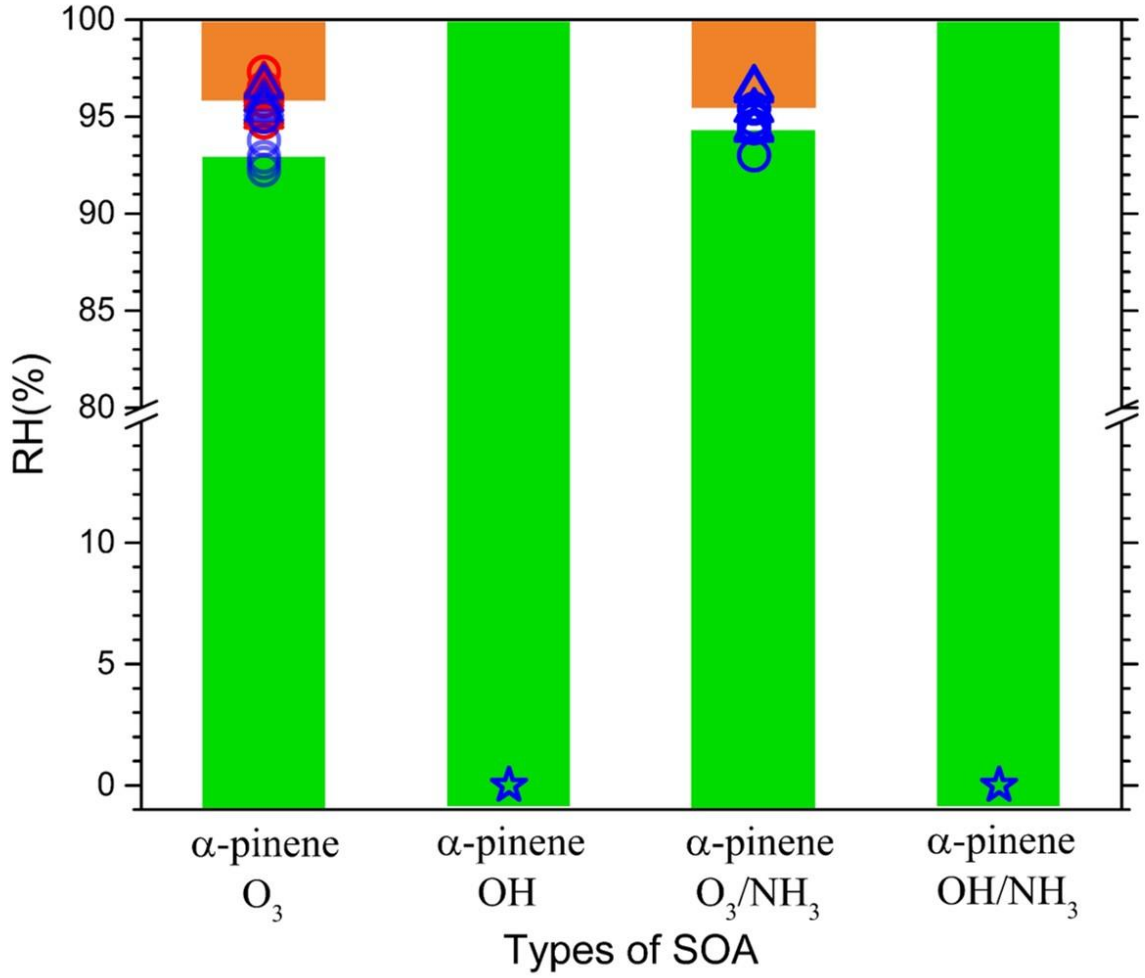

Figure 5. Relative humidity (RH) at which two phases were observed during RH scanning as a function of four different types of SOA particles. Blue and red symbols are from this study and from Renbaum-Wolff et al. (2016), respectively. Circles represent merging RH (MRH) for RH decreasing and triangles represent separation RH (SRH) for RH increasing. RH = 0 % indicates no LLPS. Green shaded region indicates one phase present and orange shaded region indicates two phases present in the SOA particles.

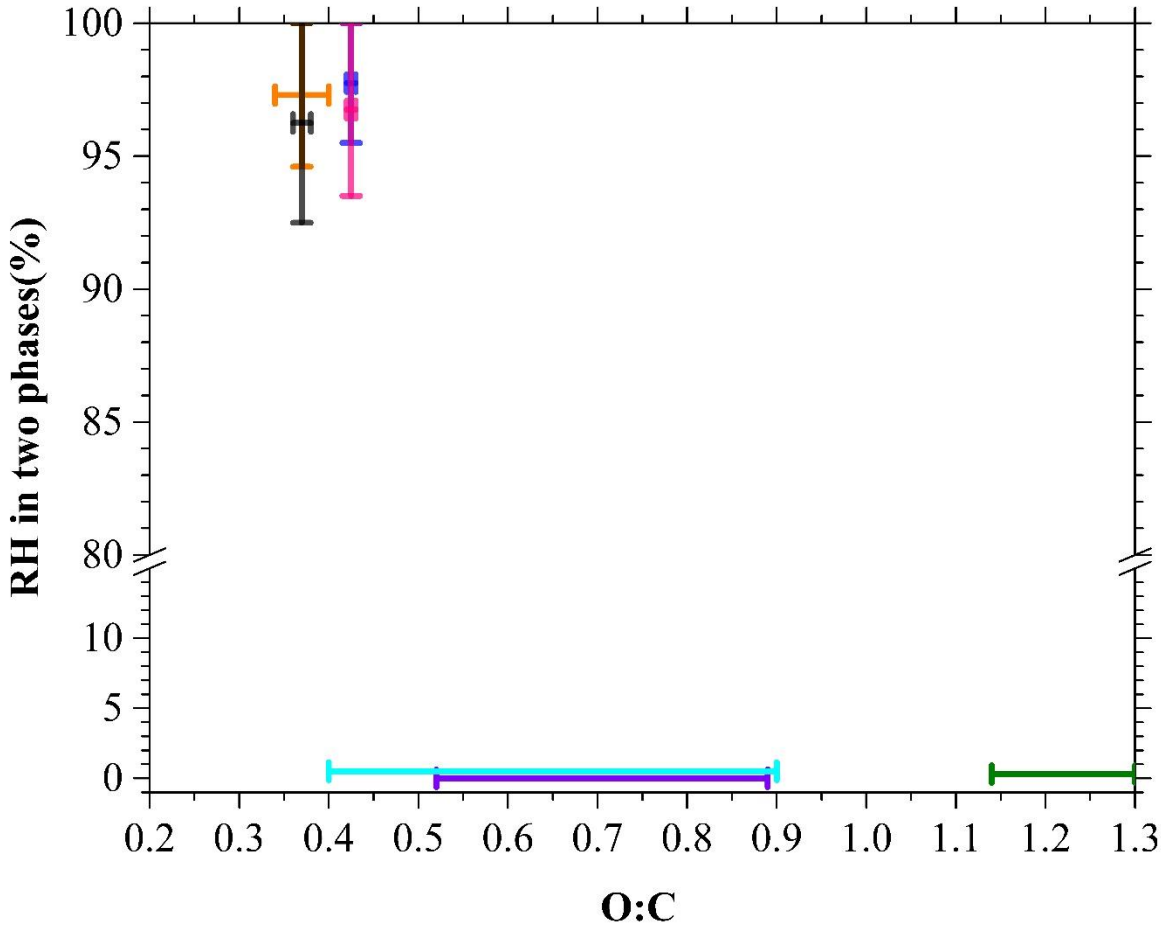

Figure 6. Relative humidity in two phases as a function of average O:C of SOA particles derived from α-pinene ozonolysis (pink) and α-pinene photo-oxidation (cyan) from this study, β-caryophyllene ozonolysis (black) from Song et al. (2017), α-pinene ozonolysis (blue) from Renbaum-Wolff et al. (2016), limonene ozonolysis (orange) from Song et al. (2017), toluene photo-oxidation (green) from Song et al. (2017), and isoprene photo-oxidation (puple) from Rastak et al. (2017). The O:C and related experimental conditions are summarized in Tables S1 and S2.